



## Structure study of GaN:Mg films by X-ray absorption near-edge structure spectroscopy

Y.C. Pan<sup>a</sup>, S.F. Wang<sup>a</sup>, W.H. Lee<sup>a</sup>, W.C. Lin<sup>a</sup>, C.I. Chiang<sup>b</sup>, H. Chang<sup>b</sup>, H.H. Hsieh<sup>c</sup>, J.M. Chen<sup>d</sup>, D.S. Lin<sup>e</sup>, M.C. Lee<sup>a</sup>, W.K. Chen<sup>a</sup>, W.H. Chen<sup>a,\*</sup>

<sup>a</sup>Department of Electrophysics, National Chiao-Tung University, Hsin-Chu, Taiwan, 300 ROC

<sup>b</sup>Chung-Shan Institute of Science and Technology, Tao-Yuan, Taiwan, 325 ROC

<sup>c</sup>Department of Physics, Tamkang University, Tamsui, Taiwan, 251 ROC

<sup>d</sup>Synchrotron Radiation Research Center, Hsin-Chu, Taiwan, 300 ROC

<sup>e</sup>Institute of Physics, National Chiao-Tung University, Hsin-Chu, Taiwan, 300 ROC

Received 13 November 2000; accepted 26 December 2000 by B. Jusserand

### Abstract

X-ray absorption near-edge fine structure (XANES) spectroscopy from N K-edge measurement was employed to examine the crystal structure of metallorganic vapor phase epitaxy (MOVPE) grown Mg-doped GaN (GaN:Mg) films. The result showed that Mg doping induced crystal stacking faults to occur at the film surface causing a fraction of hexagonal phase to transform into cubic phase. As a consequence of this, XANES spectra of the films were found to vary with the dopant concentration and to lose pure hexagonal character when examined with the incident angle  $\theta$  of the X-ray beam. Spectral characteristic variation between the two phases allows us to estimate the phase composition of the samples. The trend of increasing cubic phase component in dopant concentration is consistent with the observed Normaski optical micrograph. © 2001 Published by Elsevier Science Ltd.

**Keywords:** A. Mg-doped GaN; B. MOVPE; C. Cubic phase; E. XANES

**PACS:** 61.10.Ht; 61.72.Vv; 68.35.Bs; 78.40.Fy

Group III-nitrides are important compound semiconductors for device applications in short-wavelength light emitting and detecting, high temperature and power electronic unit, and optical data storage [1,2]. The performance of GaN-based devices is superior to other blue light-emitting ones made of SiC and ZnSe [3,4]. The group III-nitride semiconductor devices owe their success to the breakthrough of p-type doping technique, which involves selecting suitable p-type dopant source, growth condition, and method of electric activation [5–7]. Being a group IIA element, Mg has been an excellent p-type dopant for GaN films. Owing to large differences in lattice constants and thermal expansion coefficients between GaN and Al<sub>2</sub>O<sub>3</sub> substrate [8], doping GaN films has continuously been a challenging task. Epitaxial GaN films usually bear crystalline imperfections that, in turn, degrade their physical

property and device performance. The degree of degradation depends largely on the substrate type, orientation, and several other growth conditions [9,10]. Recent X-ray absorption studies of Si-doped GaN showed strong dopant effects on the local structure [11]. It is therefore believed that the incorporation of the impurity Mg atom should also show dopant effects on the local structures that can be revealed by X-ray absorption spectroscopy, in particular, the near-edge structure (XANES).

All Mg-doped GaN samples (thickness  $\sim 0.5$ – $1 \mu\text{m}$ ) used in the experiment were grown on (0001) Al<sub>2</sub>O<sub>3</sub> substrate by metallorganic vapor phase epitaxy (MOVPE) in the atmospheric pressure. Trimethylgallium (TMGa), ammonia (NH<sub>3</sub>), and bis-cyclopentadienyl-magnesium (Cp<sub>2</sub>Mg) were used as the Ga, N, and Mg sources, respectively. The carrier gas was purified nitrogen. Prior to the epilayer growth, the substrate was preheated for 10 min at 1100°C in pure N<sub>2</sub> ambience, nitridated for 2 min at 1050°C in NH<sub>3</sub>/N<sub>2</sub> surroundings and then cooled down to 520°C under about

\* Corresponding author.

E-mail address: whchen@cc.nctu.edu.tw (W.H. Chen).

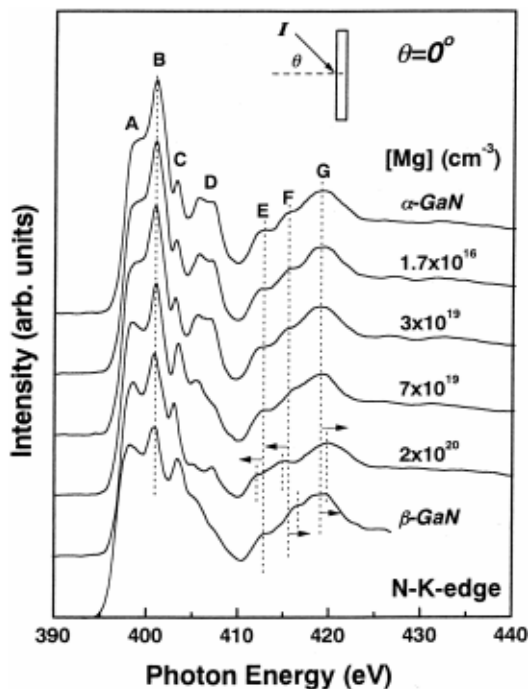


Fig. 1. N K-edge XANES spectra from undoped (0002)-hexagonal ( $\alpha$ -GaN) and various Mg-doped GaN (GaN:Mg) samples at normal incidence angle ( $\theta = 0^\circ$ ), comparing with Katsikini's cubic data ( $\beta$ -GaN) from Ref. [13].

0.7 slm  $\text{NH}_3$  and  $10.4 \mu\text{mol min}^{-1}$  TMGa flow rates for the deposition of GaN nucleation layer to about  $375 \text{ \AA}$ -thickness. After low-temperature nucleation layer deposition, the growth temperature ( $T_g$ ) and V/III ratio were fixed at  $1075^\circ\text{C}$  and 3000 for GaN epilayer growth.

The undoped GaN film clearly exhibits (0002)-hexagonal phase in XRD measurement [12]. The  $\text{Cp}_2\text{Mg}$  dopant flow rates used in the sample preparation were increased stepwise from 0 to  $0.79 \mu\text{mol min}^{-1}$  to achieve Mg concentrations of 0,  $1.7 \times 10^{16}$ ,  $1 \times 10^{19}$ ,  $3 \times 10^{19}$ ,  $7 \times 10^{19}$ , and  $2 \times 10^{20} \text{ cm}^{-3}$ . These values were estimated from secondary ion mass spectrometric data.

The X-ray absorption near-edge structure (XANES) spectra were recorded at the nitrogen (N) K-edge ( $\sim 398 \text{ eV}$ ) in the energy range of 390–445 eV using the HSGM beam-line of the Synchrotron Radiation Research Center (SRRC) in Hsin-Chu, Taiwan. The grating ( $700 \text{ lines mm}^{-1}$ ) is made of gold-coated fused silica and is suitable to cover the photon-energy range from 207 to 517 eV. The spectra were measured in fluorescence yield (FLY) mode with a high-purity and high-sensitivity seven-element Ge detector. The X-ray incident angles  $\theta$  were varied from 0 to  $80^\circ$  in four increments with respect to the substrate normal (inset of Fig. 1). The samples were kept at room temperature under a chamber pressure of better than  $5 \times 10^{-9}$  torr. The resolution of the spectra was better than 0.2 eV.

Fig. 1 shows N K-XANES spectra for undoped hexagonal ( $\alpha$ -GaN) and the four different Mg-doped GaN (GaN:Mg) samples measured at the normal incident angle ( $\theta = 0^\circ$ ). All spectra were normalized to unit absorption with a linear pre-edge background removal and to the atomic limit. The cubic GaN ( $\beta$ -GaN) taken from Katsikini et al. [13] is included in Fig. 1 for comparison. We designate the distinct absorption peaks with letters from A to G for easier discussion. Among them, peaks A, B, C and D represent the transitions from nitrogen 1s core electrons to partial (p-like) density of unfilled states in the conduction band [13]. As Fig. 1 depicts, peaks A, B, C, and D remain in almost the same energy positions but their intensities strongly vary with the dopant concentration. Comparing to the normalized peak A, the

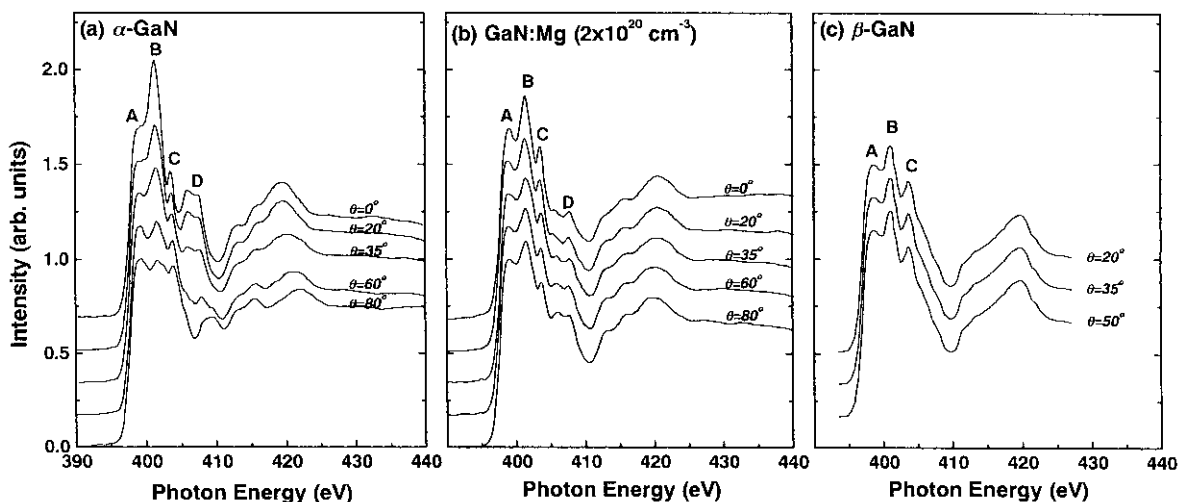


Fig. 2. The angle-dependent XANES spectra for the three difference samples: (a) hexagonal; (b) heavily Mg-doped ( $[\text{Mg}] \sim 10^{20} \text{ cm}^{-3}$ ), and (c) cubic GaN (Katsikini's data) samples.

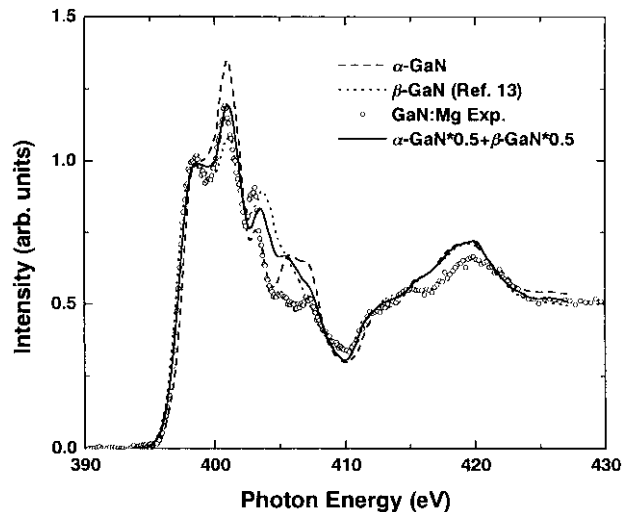


Fig. 3. Fitting curve (solid line) of the experimental XANES spectrum from the heaviest Mg-doped GaN (open circles) as a weighted average of the spectra of the hexagonal (dash line) and the cubic (dot line, Katsikini's data) samples. The weighted average factors are 0.5 and 0.5, respectively. All the spectra curves taken at normal angle ( $\theta = 0^\circ$ ).

intensity of peak C increases with the Mg concentration, whereas those of B and D decrease. The similar tendency was also observed in the mixed phase structure GaN samples reported by Katsikini et al. [13]. The observed movements in peaks in our GaN:Mg may well be interpreted as the modification of the N partial density of unoccupied states in conduction band by the incorporation of Mg impurity [13]. The intensity of peaks E, F, and G, however, weakly depend on the Mg concentration. It is worth noticing that peaks F and G exhibit a strong position difference for  $\alpha$  and  $\beta$  phase structure. This trend also was reported by Lübke et al. [14]. Nonetheless, peak F shifted in the opposite direction when compared to that of  $\beta$ -GaN. As the Mg impurity concentration increases to  $2 \times 10^{20} \text{ cm}^{-3}$ , the energy position of peaks E and F shift toward low-energy positions whereas peak G toward high-energy positions. Except for peak E, the shifting behavior of peaks F and G in our samples was similar to that reported by Lübke et al. [14]. These small inconsistencies in energy shifts may be, in part, due to the weakness and broadness of these peaks or may be due to the different methods or parameters used in growing these samples.

The general inference we draw from Fig. 1 is the change of spectral response from hexagonal ( $\alpha$ -GaN) to cubic ( $\beta$ -GaN) as the dopant concentration increases. Thus, the spectral resemblance of the highest Mg content sample to  $\beta$ -GaN is the greatest suggesting the highest degree of crystal phase mixing in all. Since XANES spectra are sensitive to the group symmetry of the sample as well as the local structure around the absorbing atom, we also performed the angle varying measurements of the samples. Fig. 2(a) shows the angular dependent XANES from  $\alpha$ -GaN. When the intensity of the peak A is normalized, the magnitude of

peaks B and D decrease and as the Mg dopant concentration increases, the magnitude of peak C increases. The N K-XANES spectra of the lightly Mg-doped samples ( $[\text{Mg}] < 10^{17} \text{ cm}^{-3}$ ) resemble those of undoped  $\alpha$ -GaN in Fig. 2(a) owing to the dominant hexagonal phase. In contrast to the undoped or lightly Mg-doped GaN, angular dependent XANES spectra of the heavily doped sample in Fig. 2(b) show great reduction of angular dependency in these spectra. In fact, they come to more resemble the  $\beta$ -GaN sample in Fig. 2(c), suggesting a high fraction of cubic structure in the films.

According to studies of impurity-doping effects in group IV and III–V compound semiconductors such as Si:Fe [15], Si:Ge [16], and GaAs:Si [17,18], stacking faults are easily induced by impurity doping. These stacking faults, in turn, cause local structural changes. For example, the original hexagonal structures of SiC, ZnS, CdI<sub>2</sub>, and CdBr<sub>2</sub> were found to be modified when doped with impurities like N, P, Al, and B [19]. From the crystal structure viewpoint, the hexagonal stacking sequence ABAB ... and cubic one ABCABC ... are very close. The theoretical calculation of Yeh et al. pointed out that the difference in formation energies for both stacking sequences is only about  $10 \text{ meV atom}^{-1}$  [20]. It is, therefore, quite possible for Mg impurity in GaN to induce local structure changes by stacking faults, which then resulted in crystal phase mixing of the samples.

In our study of GaN grown on (0001) sapphire at different temperatures, we have found substantial changes of photoluminescence (PL), Raman shift, and X-ray diffraction (XRD) patterns occurring around a boundary temperature of  $750^\circ\text{C}$  [21]. We attributed these changes to different dominant crystal polytypes formed during the growth.

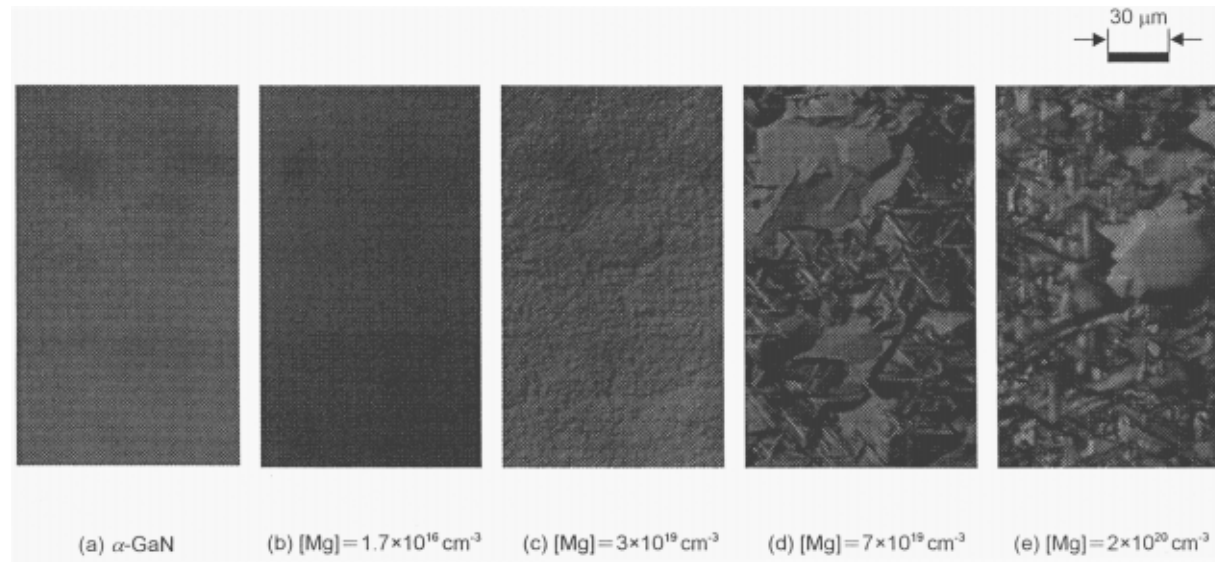


Fig. 4. The Normaski optical micrographs of (a) undoped hexagonal ( $\alpha$ -GaN) and Mg-doped GaN samples in Mg solid concentration of (b)  $1.7 \times 10^{16}$ , (c)  $3 \times 10^{19}$ , (d)  $7 \times 10^{19}$ , and (e)  $2 \times 10^{20} \text{ cm}^{-3}$ .

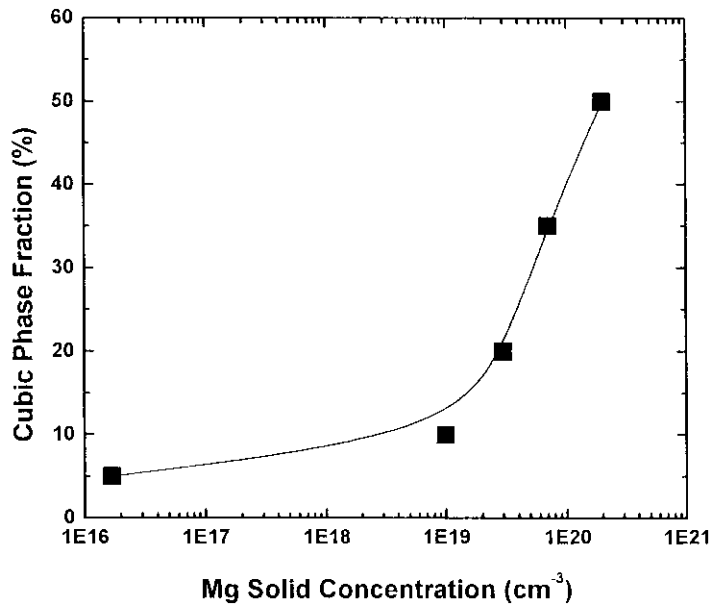


Fig. 5. The variations of cubic fraction expressed in mixing ratio  $x$  with Mg concentration from  $1.7 \times 10^{16}$  to  $2 \times 10^{20} \text{ cm}^{-3}$ . A steeper slope was observed to commence from approximately  $5 \times 10^{19} \text{ cm}^{-3}$ .

GaN grown at temperatures higher than  $750^\circ\text{C}$  favors the formation of the hexagonal polytype and lower than  $750^\circ\text{C}$ , on the other hand, the cubic polytype. As we have stated, our GaN:Mg samples were grown at  $1075^\circ\text{C}$ , a temperature that favors the hexagonal polytype. It is of interest to see that owing to Mg doping, GaN films grown at  $1075^\circ\text{C}$  still permit the cubic polytype to form and mix with the hexagonal one. The mixing ratio  $x$  of the two phases, taking our highest Mg content sample for example, can be estimated with the aid of the  $\beta$ -GaN data we borrowed and displayed in Fig. 1 using the following absorption intensity equation  $y = \text{cubic} \times x + \text{hexagonal} \times (1 - x)$ . The result is given in Fig. 3 and the value of  $x$  is determined to be  $\sim 0.5$  as the data running through the middle of peaks B of the two polytypes. Such a high cubic phase fraction seems dubious at the first glance, since the overall bulk XRD and Raman data still indicated hexagonal domination [12]. The recurrence of Raman 535 and  $555 \text{ cm}^{-1}$  cubic TO modes [21] and the broadening of  $2\theta = 34.5^\circ$  peak of the (0002) XRD were found in high Mg content samples [12]. They did signify the presence of cubic structure, but did not allow us to estimate the mixing ratio  $x$ . However, if we examine the surface morphology and the nature of the surface-sensitive fluorescence character, we can argue this high-phase mixing ratio is quite possible. Fig. 4 shows the optical micrographs of the samples. We see as Mg solid concentration increases, the homogenous and mirror-like surface gradually becomes rough and non-uniform and even grows many triangle-like structures on high Mg flow rate samples. These triangular structures are akin to those observed by Cros et al. [22]. Their micro-Raman data and high-resolution TEM measurements

concluded these triangular structures were related to cubic phase. Considering XANES data are contributions from only  $\sim 100 \text{ \AA}$ -deep specimen region, we believe the recorded fluorescence signal almost represents the structural property of these triangular plateaus. Another independent support to the high mixing ratio, as we have shown, came from the insignificant disparity among the spectra measured in different angles (Fig. 2) and the similarity of them to the  $\beta$ -GaN spectrum. Samples containing less Mg concentrations with their mixing ratio  $x$  determined by the same equation with the aid of the same cubic data indeed showed smaller  $x$  values. Fig. 5 depicts the trend curve of increasing mixing ratio with increasing Mg concentrations. It is seen when the Mg concentration reached the neighborhood of  $5 \times 10^{19} \text{ cm}^{-3}$   $x$  value started to increase abruptly. This steeper slope region matches the last two pictures of Fig. 4 representing a rough surface with random distribution of the triangular plateaus. The increasing number of triangular plateau degrades the film quality and, additionally, affects the p-type Mg activation efficiency as other researchers have found [23].

Comparison of N K-XANES spectra from different dopant concentrations of GaN:Mg using fixed incident angle ( $\theta = 0^\circ$ ) revealed a Mg-dependent variation of the absorption profiles, which vary towards increasing  $\beta$ -GaN resemblance in increasing Mg concentration. Comparison of N K-XANES spectra from  $\alpha$ -GaN taken at different incident angles demonstrated the anisotropic hexagonal character of the samples. Comparison of N K-XANES spectra from the highest Mg content GaN:Mg film measured at different incident angles showed minimal angular dependence with

the overall profile resembling that of  $\beta$ -GaN. Based on these findings, we assert that GaN cubic polytype can be formed during the impurity doping of Mg even at  $T_g = 1075^\circ\text{C}$ . For our samples, a mixing ratio of as high as  $x \approx 0.5$  between the two phases was reached when the  $\text{Cp}_2\text{Mg}$  flow was about  $0.79 \mu\text{mol min}^{-1}$  (corresponding to Mg concentration of  $\sim 2 \times 10^{20} \text{ cm}^{-3}$ ).

### Acknowledgements

The authors would like to thank the National Science of the Republic of China for the financial support for this research under contract numbers NSC88-2112-M009-021, -022, and -031.

### References

- [1] H. Morkoc, S. Strite, G.B. Gao, M.E. Lin, B. Sverdlov, M. Burns, *J. Appl. Phys.* 76 (1994) 1363.
- [2] S. Nakamura, M. Senoh, S. Nagahama, N. Iwasa, T. Yamada, T. Matsushita, H. Kiyoku, Y. Sugimoto, *Appl. Phys. Lett.* 68 (1996) 2105.
- [3] Y. Matsushita, K. Koga, Y. Ueda, T. Tamaguchi, Oyo Buturi 60 (1991) 159.
- [4] H. Katayama-Yoshida, T. Yamamoto, Proc. of German–Japanese Seminar on II–VI semiconductors in Bremen, 23–27 March 1997, *Phys. Status Solidi (B)* 202 (1997) 763.
- [5] M. Kunzer, J. Baur, U. Kaufmann, J. Schneider, H. Amano, I. Akasaki, *Solid State Electron.* 41 (1997) 189.
- [6] H. Tokunaga, I. Waki, A. Yamaguchi, N. Akutsu, K. Matsumoto, *J. Cryst. Growth* 189/190 (1998) 519.
- [7] S. Nakamura, N. Iwasa, M. Senoh, T. Mukai, *Jpn J. Appl. Phys.* 31 (1992) 191.
- [8] I. Akasaki, H. Amano, Y. Koide, K. Hiramatsu, N. Sawaki, *J. Cryst. Growth* 98 (1989) 209.
- [9] T. Lei, M. Fanciulli, R.J. Molnar, T.D. Moustakas, R.J. Graham, J. Scanlon, *Appl. Phys. Lett.* 59 (1991) 944.
- [10] T.S. Cheng, L.C. Jenkins, S.E. Hooper, C.T. Foxon, J.W. Orton, D.E. Lacklison, *Appl. Phys. Lett.* 66 (1995) 1509.
- [11] Z.H. Lu, T. Tylliszczak, P. Broderson, A.P. Hitchcock, J.B. Webb, H. Tang, J. Bardwell, *Appl. Phys. Lett.* 75 (1999) 534.
- [12] Y.C. Pan, Doctoral thesis from National Chaio Tung University, 2000, unpublished data.
- [13] M. Katsikini, E.C. Paloura, T.D. Moustakas, *J. Appl. Phys.* 83 (1998) 1437.
- [14] M. Lübbe, P.R. Bressler, W. Braun, T.U. Kampen, D.R.T. Zahn, *J. Appl. Phys.* 86 (1999) 209.
- [15] J. Jablonski, M. Saito, Y. Miyamura, M. Imai, *Jpn J. Appl. Phys.* 35 (1996) 520.
- [16] A. Gupta, M.M. Rahman, J. Qiao, C.Y. Yang, S. Im, N.W. Cheung, P.K.L. Yu, *J. Appl. Phys.* 75 (1994) 4252.
- [17] D.G. Lin, J.C. Fan, C.P. Lee, K.H. Chang, D.C. Lion, *J. Appl. Phys.* 73 (1993) 608.
- [18] W.G. Opyd, J.F. Gibbons, A.J. Mardinly, *Appl. Phys. Lett.* 53 (1988) 1515.
- [19] G.C. Trigunayat, *Solid State Ionics* 48 (1991) 3.
- [20] C.-Y. Yeh, Z.W. Lu, S. Froyen, A. Zunger, *Phys. Rev. B* 46 (1992) 10087.
- [21] H.C. Lin, J. Ou, W.K. Chen, W.H. Chen, M.C. Lee, *Jpn J. Appl. Phys.* 36 (1997) L598.
- [22] A. Cros, R. Dimitrov, H. Angerer, O. Ambacher, M. Stutzmann, S. Christiansen, M. Albrecht, H.P. Strunk, *J. Cryst. Growth* 181 (1997) 197.
- [23] C.R. Lee, J.Y. Leem, S.K. Noh, S.E. Park, J.I. Lee, C.S. Kim, S.J. Son, K.Y. Leem, *J. Cryst. Growth* 193 (1998) 300.